Microalgae Separation by Inertia-enhanced Pinched Flow Fractionation

Saijie Wang,[1] Zhijian Liu,[2,*] Sen Wu,[2] Hongyan Sun,[3] Wu Zeng,[2] Jintao Wei,[4] Zixiao Fan,[2] Zhuohang Sui, [2] Liankun Liu,[2] and Xinxiang Pan,[2,5]

[1] School of Science, Dalian Maritime University, Dalian, China.

[2] College of Marine Engineering, Dalian Maritime University, Dalian, China.

[3] School of Maritime Economics and Management of Dalian Maritime University, Dalian Maritime University, Dalian, China.

[4] Maritime College, Dalian Maritime University, Dalian, China.

[5] College of Navigation, Guangdong Ocean University, Zhanjiang, China.

*Correspondence should be addressed to the following author:

Zhijian Liu (Associate Professor)

College of Marine Engineering

Dalian Maritime University

Dalian, China

liuzhijian@dlmu.edu.cn

Keywords: iPFF; microalgae; microfluidic chip; separation

Abbreviations: iPFF

Abstract

To improve the accuracy and efficiency of ships' ballast water detection, the separation of microalgae according to size is significant. In this paper, a method to separate microalgae based on inertia-enhanced pinched flow fractionation (iPFF) was reported. The method utilized the inertial lift force induced by flow to separate microalgae according to size continuously. The experimental results show that, as the Reynolds number increases, the separation effect becomes better at first, but then stays unchanged. The best separation effect can be obtained when the Reynolds number is 12.3. In addition, with the increase of the flow rate ratio between sheath fluid and microalgae mixture, the separation effect becomes better and the best separation effect can be obtained when the flow rate ratio reaches 10. In this case, the recovery rate of *Tetraselmis* sp. is about 90%, and the purity is about 86%; the recovery rate of *Chlorella* sp. is as high as 99%, and the purity is about 99%. After that, the separation effect keeps getting better but very slowly. In general, this study provides a simple method for the separation of microalgae with different size, and lays a foundation for the accurate detection of microalgae in the ballast water.

1 Introduction

The discharge of the microalgae in the ships' ballast water from one port to the others during the international trade, is one of the main causes of biological invasion [1]. It is necessary to detect microalgae before the discharge of the ship's ballast water into the sea [2]. However, there are many kinds of microalgae in the ballast water and they have a wide range of sizes. So it is a great challenge to detect these microalgae directly as every detection method has a certain size detection interval. In order to solve that, the separation of microalgae according to size before detecting is necessary.

In the last decades, the research on the microalgae separation is popular and many methods have been proposed and developed. Based on whether an external physical field is needed, these methods fall into two categories: active separation and passive separation [3]. The former one often requires external physical fields, such as electric field, magnetic field, and sound field [4-6]. The technique based on electrophoresis or dielectrophoresis can separate microalgae cells according to their different volumes or dielectric constants. Recently, Jiang et al. developed a recycling free-flow isoelectric focusing method based on electrophoresis to achieve the enrichment of low-abundant bacteria [7]. This method successfully increased the bacterial abundance by 225%. Dong et al. developed a free-flow electrophoresis (FFE) technique and separated Escherichia coli and Staphylococcus aureus effectively. This work provided a new idea for cell separation [8]. Similarly, He et al. separated complete mitochondria from mitochondria resuspension buffer using the method of free-flow isoelectric focusing. This method has advantages in measuring the isoelectric point of substances such as proteins [9]. Xuan et al. have used the technique based on magnetic field to successfully separate polystyrene particles of 3 and 10 μm [10]. In addition, immuno-magnetic beads are usually used for the separation of tumor cells or exosomes [11]. It can separate high purity target cells and other substances from complex mixtures. The sound field

separation method is mainly based on high frequency sound waves. Dow et al. isolated and purified bacteria from the blood using acoustic method, which greatly increased the detection limit of *Escherichia coli* [12]. However, the external force fields required in the active separation may bring harm to the activity of bio-particles, which limits the development of this method in the field of microalgae separation [4]. So the researchers turn to the passive separation which does not require an external physical field. Centrifugation is the most common separation method. However, it is difficult to be integrated with microfluidic chips [13]. There are also some methods typically exploit special flow channel structures to separate microalgae based on their size. The separation technologies of inertial microfluidics based on channel innovations have been recognized as a powerful tool for high throughout microalgae separation. The separation of *Chlorella* sp. and *Cosmarium* sp. using dean flow in a spiral microfluidic device was reported by Lee et al. [14]. This technique has a high flux and simple structure because it only needs pressure-driven. Nevertheless, the technique can only separate the diluted sample due to the interaction between among cells. Recently, Li et al. reported a sinusoidal-shaped inertial microfluidic device to purify cancer cells [15]. Warkiani ME et al. proposed a spiral-shaped inertial microfluidic channel to separate tumor cells from urine [16].

Specially, a method named pinched flow fractionation (PFF) utilizing the laminar flow profile in microchannel to separate particles by size continuously was proposed by Yamada et al. [17]. On a PFF microfluidics, particles with different size must be focused to one sidewall of channel by using a pressure-driven sheath flow. The particles, as a result, locate at the different streamlines that are dominated by the size. Further, the distance between particles with different size is enlarged at the downstream abruptly broadened part. However, PFF can only work normally at a larger flow rate ratio, and the separation distance in the abruptly broadened part is very limited [18]. Recently, Inertia-Enhanced Pinched Flow Fractionation

technique (iPFF) based on PFF was firstly proposed by Xuan et al. to improve the separation effect of PFF [18, 19]. The method exploits the inertial lift force, an additional force induced by flow, to enhance the polystyrene particles offset in PFF and consequently increases the separation effect. Compared with PFF, iPFF can work normally at a lower flow rate ratio, so a higher particle flux can be obtained, which can be increased by at least 10 times. Besides, the separation distance in the abruptly broadened part is also significantly improved [18]. Compared with the existing inertial microfluidics technology, iPFF has the advantages of high separation efficiency and high operational throughput. What is more valuable is that this method hardly causes any damage to the cells. However, the application of iPFF in microalgae cells separation has not been studied systematically.

The purpose of this paper is to demonstrate the potential application of iPFF technique for microalgae separation in ballast water. In addition, the effects of fluid inertia (Re) and flow rate ratio (α) on the separation effect are explored systematically, and the optimal separation parameters are obtained for the separation of *Chlorella* sp. and *Tetraselmis* sp.

2 Materials and Methods

2.1 Separation system

The microalgae separation system, shown in Figure 1A, consists of a microfluidic chip, a microscopy (not drawn in the figure 1A), two micro-injection pumps, two syringes, and some rigid Teflon capillaries for connecting the syringes and microfluidic chip.

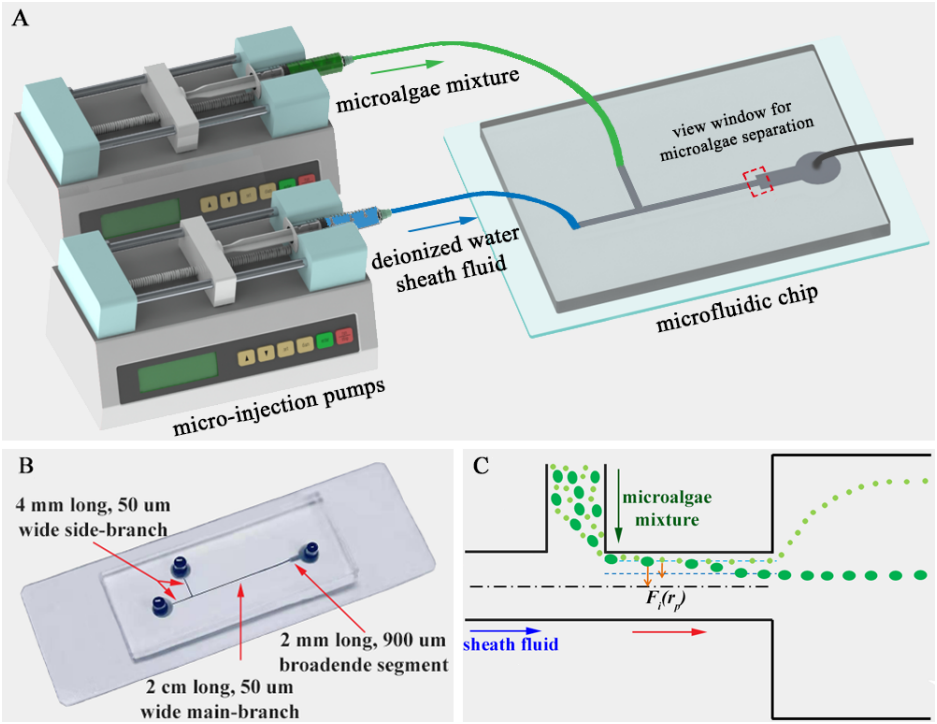

Figure 1. The diagram of the microalgae separation system (A)and the microfluidic chip (B) designed for the experiment. The chip is filled with black ink for clarity. The schematic diagram of the microalgae separation via iPFF is drawn not scale (C). The inertial lift forces are indicated by Fi. The solid arrows indicate the flow direction in the sheath flow (blue), microalgae mixture (green) and main channel (red).

As shown in Figure 1B, the microfluidic chip was designed with two inlet wells, one outlet well, two side branch channels and one main channel. The length and width of the side branch channels are 4 mm and 50 μm, respectively, and that of the main channel are 20 mm and 50 μm, respectively. At the end of the main channel, there is an abruptly broadened segment with 2 mm in length and 900 μm in width. The overall height of the microchannel is 20 μm. It should be noted that the abruptly broadened segment is designed for further separating cells and it also serves as the observing window. A microscopy (Nikon Eclipse TE2000U, Nikon Instruments) is located just above the observing window monitoring the separation effect. Driven by the pumps (Harvard Apparatus, Pump 11 Pico Plus), the syringes

(Ordinary medical syringe with a specification of 1 mL) deliver the sample to the microfluidic chip.

2.2 Chip fabrication and sample preparation

The mold for microchannel was fabricated on a silicon substrate (4″N/PHOS, Montco Silicon Technology Inc., Spring City, PA, USA) using a mask-less laser writing machine (MLA150, Heidelberg instruments, Germany) [20, 21]. Afterwards, the polydimethylsiloxane (PDMS, Sylgard 184, Dow Corning, USA) was mixed with the curing agent in a weight ratio of 10: 1 and degassed [21]. Then, the mixture was poured on the silicon mold and baked in an oven (Isotemp model 280A, Fisher Scientific, Pittsburgh, PA, USA) at 70 ℃ for 4 hours to keep full curing [22]. After that, the PDMS was peeled off and perforated separately in the inlet and outlet wells with a hole punch. Finally, the PDMS together with a clean glass slide (25.66 × 75.47 × 1.07 mm, CITOGLAS, China) was put into a plasma cleaner (HARRICK PLASMA, Ithaca, NY, USA) and processed for 100s. The irreversible combination of the two would produce a microfluidic chip.

The *Chlorella* sp. and *Tetraselmis* sp. used in the experiment were bought from Shanghai Guangyu Biological Technology Co., Ltd. The shape and size of the microalgae were examined by an optical microscopy. As the microalgae were in different growth stages, their sizes were distributed in a range. Specially, *Chlorella* sp. are spherical, whose equivalent diameter varies from 3 μm to 5 μm. *Tetraselmis* sp. are flat, of which, the average length and width, are approximately 11-14 μm and 7-9 μm, respectively. To remove impurities from the microalginogen solution, the samples were washed by a centrifuge with the speed of 5000 r/min for more than three times. After washing, mix two microalgae solution and keep shaking for one minute to obtain a uniform mixed solution of *Chlorella* sp.

and *Tetraselmis* sp.. The final concentration of the microalgae used in this study is about 6.0 $\times 10^4$ cells/mL.

2.3 Experimental method

The microalgae mixture solution and deionized water were firstly sucked into two syringes, respectively. Then, the syringes were fixed on the micro-injection pumps and connected to the inlet wells on the microfluidic chip by Teflon capillaries. After that, the pumps were turned on to drive the sample (both the microalgae mixture solution and deionized water) into the side branch channels in the microfluidic chip. To avoid the microalgae entering the sheath fluid channel, the deionized water was driven before the microalgae mixture. The outlet well on the chip was connected to a waste bottle by capillaries. The separated results of *Chlorella* sp. and *Tetraselmis* sp. could be viewed at the abruptly broadened segment using an inverted microscope (Nikon Eclipse TE2000U, Nikon Instruments) with a CCD camera (Nikon DS-QilMc). It should be noted that the separation effect was recorded only when the system was stable. When studying the effects of the fluid inertia and the flow rate ratio, the pumps were adjusted directly to the desired value without changing syringes and microfluidic chip. The streak images were obtained by superimposing a sequence of about 4500 images with the Matlab2016a software [18]. The percentage distribution of microalgae cells was calculated by the software ImageJ which was used to divide the abruptly broadened segment of the series of images into 20 parts longitudinally and count the number of cells in each part separately. The diagrams were processed by the Origin Pro 2020.

3 Results and Discussion

3.1 Theoretical analysis

The mechanism of iPFF is schematically shown in Figure 1C. The microalgae mixture is firstly focused to one sidewall using a sheath fluid flow at the T-shaped channel. Then, the inertial lift force induced by flow [23-26], F_i, pushes the microalgae toward the center of the channel. It should be noted that, F_i can be calculated as following:

$$F_i = C_L \rho r_P^4 \gamma^2 \quad (1)$$

Where C_L is a dimensionless lift coefficient which is a dominated by the Re and the position of the microalgae, ρ is the density of the sample fluid, r_P is the equivalent radius of the microalgae, and γ is the shear rate. Obviously, F_i is a strong depend on the cell size and the lateral offset between microalgae with different size can be increased in a larger interval. In addition, the separation distance between microalgae was further enlarged in the abruptly broadened segment [18].

There are two defined dimensionless numbers in this iPFF technique that can affect the separation effect significantly [27-30]. The first one is the Reynolds number, Re, defined as the ratio of the inertial force to the viscous force, as it dominates the inertial migration of the cells in confined channel flows [31, 32]. The Re could be as following,

$$Re = \frac{\rho U_f D_h}{\mu} = \frac{2\rho Q}{\mu(w+h)} \quad (1)$$

Where U_f is the average velocity of the fluid in the main channel, D_h is the hydraulic diameter, for the rectangular cross-section flow channel D_h can be estimated as $D_h = 2wh/(w+h)$ with h and w indicating the height and width of the rectangular channel, and Q is the flow rate in volume. The second important dimensionless number is the flow

193 rate ratio (α), which characterizes the ratio of the volumetric flow of the sheath fluid,
194 Q_{sheath}, to that of the microalgae mixture $Q_{microalgae}$, in the two side branch channels. It
195 indicates the strength of the focusing effect and affects the cell dispersion in the abruptly
196 broadened segment. Obviously, $Q = Q_{sheath} + Q_{microalgae}$.

197 3.2 The Effect of Fluid Inertia (Re)

198 As mentioned in Section 2, the Reynolds number has a large impact on the separation.
199 The effects of the Reynolds number were studied by changing the total flow rate in the main
200 channel when the flow rate ratio between the sheath fluid and the microalgae mixture was
201 fixed to 10 approximately. The experimental results are shown in Figure 2. The left part of
202 each picture is the cell streak image obtained at the abruptly broadened segment, and the light
203 color part is *Chlorella* sp., the deep color part is *Tetraselmis* sp. The right part of each picture
204 shows the percentage distribution of microalgae cells in different locations, and the blue bars
205 represent the percentage distribution of *Chlorella* sp., the red bars represent that of
206 *Tetraselmis* sp. It demonstrates that the *Chlorella* sp. can be separated from the *Tetraselmis*
207 sp. when the Reynolds number increase to 12.3 (Figure 2C). However, the separation effect
208 seems not to raise with further increasing the Reynolds number.

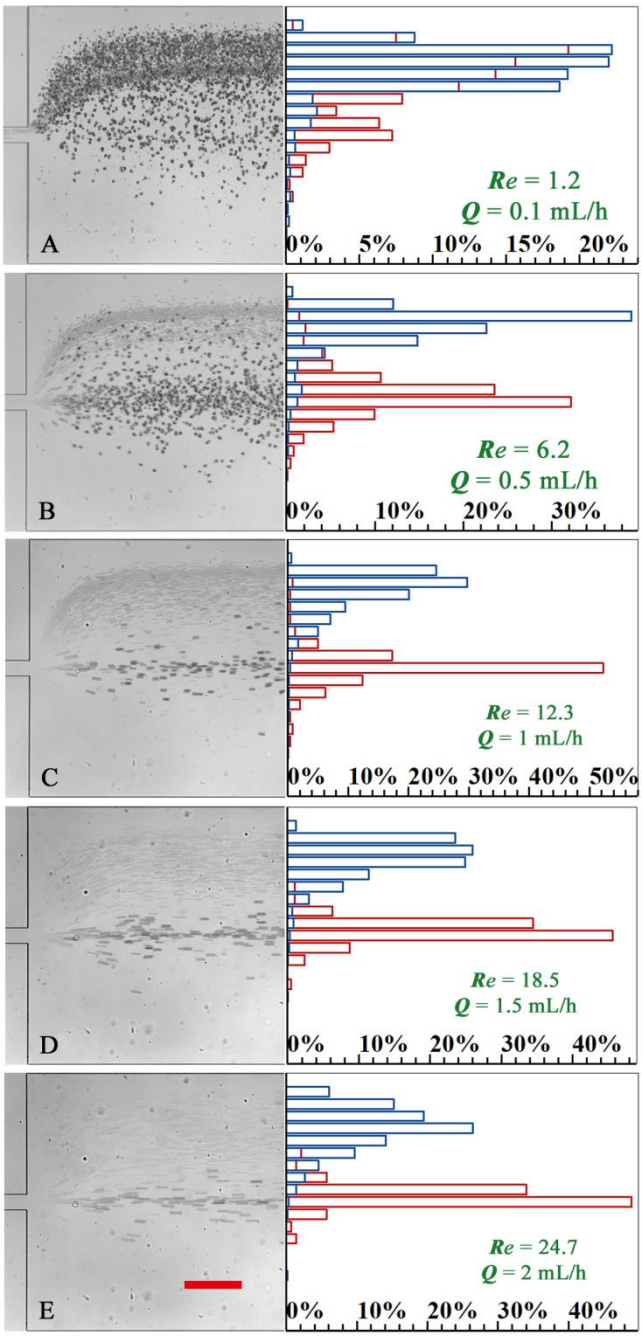

Figure 2. The effects of the fluid inertia (*Re*) on the separation of the *Chlorella* sp. and the *Tetraselmis* sp. via iPFF while *Re* increase from 1.2 (A) to 6.2 (B), 12.3 (C), 18.5 (D), and 24.7 (E). The left part of each figure is the images at the abruptly broadened segment. The light color part is *Chlorella* sp., the deep color part is *Tetraselmis* sp. The right part of each figure is percentage distribution of microalgae cells in different locations. The blue bars represent the percentage distribution of *Chlorella* sp. and the red bars represent that of *Tetraselmis* sp. The flow rate ratio between sheath fluid and microalgae mixture is maintained at 10 approximately. Cells flow from left to right in all images. The scale bar represents 200 μm.

To further analyze the separation effects, using the cell deflection from the bottom wall to determine the cell stream position [31], and a quantitative analysis of the two cell streams at the abruptly broadened segment was performed, as shown in Figure 3. The effect of the *Re* on the separation could be concluded as following. When the Reynolds number is less than 12.3 (the total flow rate is less than 1 mL/h), the widths of the cell streams decrease regularly with the increase of the Reynolds number. When the Reynolds number increases to 12.3, which means the widths of the cell streams reach the minimum, the *Chlorella* sp. and the *Tetraselmis* sp. can be completely separated at this condition. After that, as the Reynolds number further increases, the width of the cell stream of *Chlorella* sp. begins increasing, but that of *Tetraselmis* sp. continues to decrease. As a result, the separation effect basically remains unchanged. In summary, as the Reynolds number in the microchannel increases, the separation effect becomes better at first, and then remains largely unchanged.

When the Reynolds number increases from 1.2 to 12.3 (the total flow rate reaches 1 mL/h), the flow-induced inertial lift force is enhanced so much that it will push the *Tetraselmis* sp. toward the main channel centerline. Meanwhile, the lift force acting on the *Chlorella* sp. is still low due to their much smaller size and it cannot push the *Chlorella* sp. toward the central flow line. Therefore, the *Chlorella* sp. and the *Tetraselmis* sp. can be completely separated in this condition. However, when the Reynolds number further increase over 12.3, the flow-induced inertial lift force acting on the *Chlorella* sp. is also enhanced and the *Chlorella* sp. will toward to the central line. Hence, the separation distance between the *Chlorella* sp. and the *Tetraselmis* sp. decreases and the separation effect is not desirable.

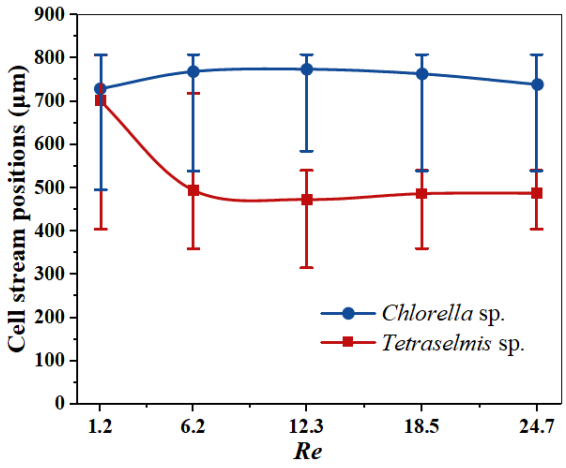

Figure 3. The effects of the fluid inertia (*Re*) on the stream positions for the *Chlorella* sp. (blue circle) and *Tetraselmis* sp. (red square). The bottom sidewall of the channel expansion was used as the reference point (0 μm). Error bars were included for both cells in Figure 2 to cover the span of each cell stream. Confidence interval of the graph is 95%.

3.3 The Effect of Flow Rate Ratio (α)

The influence of the flow rate ratio (α) on the separation effect is as important as Re . The effects of the flow rate ratio were also studied by changing the ratio between the sheath fluid flow and the microalgae mixture flow when the Reynolds number was fixed to 12.3 approximately. The experimental results are shown in Figure 4. Similar to Figure 2, the left part of each picture is the cell streak image obtained at the abruptly broadened segment and the right part shows the percentage distribution of microalgae cells in different locations. It is obvious that *Chlorella* sp. can be separated from the *Tetraselmis* sp. when the flow rate ratio increases to 10 (Figure 4D). In this case, the recovery rate of *Tetraselmis* sp. is about 90%, and the purity is about 86%; the recovery rate of *Chlorella* sp. is as high as 99%, and the purity is about 99%.

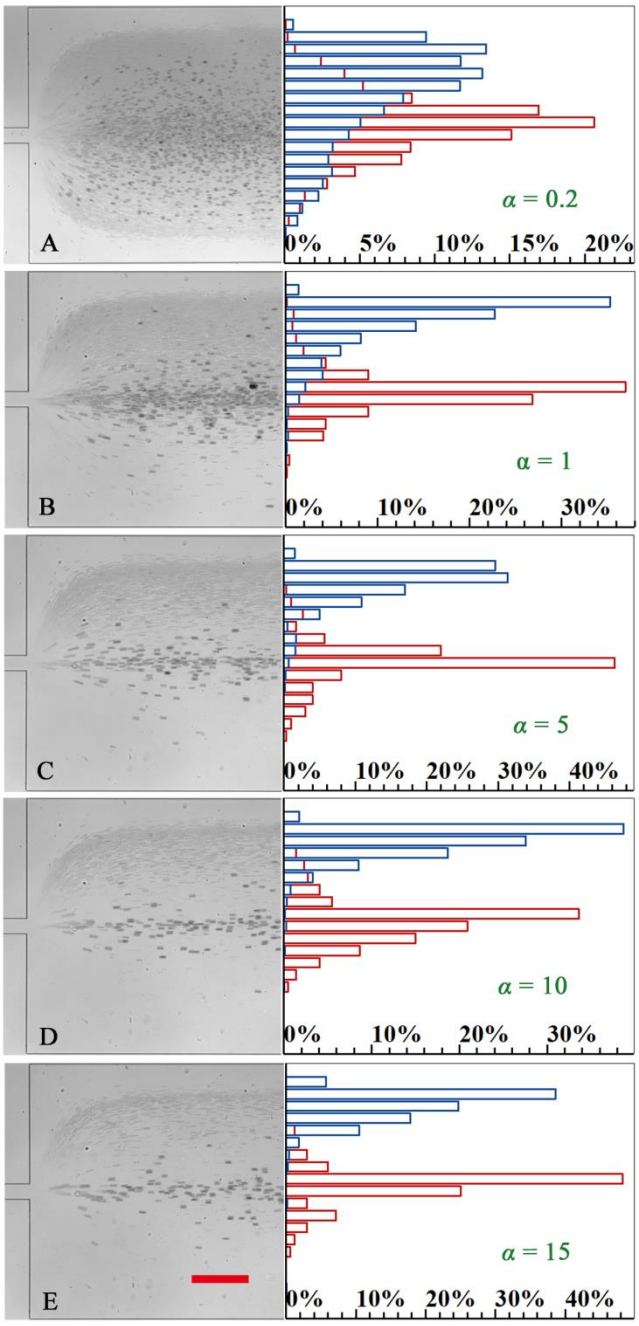

Figure 4. The effects of the flow rate ratio (α) on the separation of *Chlorella* sp. and *Tetraselmis* sp. via iPFF while α increase from 0.2 (A) to 1 (B), 5 (C), 10 (D), and 15 (E). The left part of each figure is superimposed images at the abruptly broaden segment. The light color part is *Chlorella* sp., the deep color part is *Tetraselmis* sp. The right part of each figure is percentage distribution of microalgae cells in different locations. The blue bars represent the percentage distribution of *Chlorella* sp. and the red bars represent that of *Tetraselmis* sp. The Reynolds number (*Re*) in the main channel is maintained at 12.3 approximately. Cells flow from left to right in all images. The scale bar represents 200 μm.

A quantitative analysis of the exiting positions of the two cell streams at the abruptly broaden segment is also shown in Figure 5. When the flow rate ratio (α) is below 1, the *Chlorella* sp. and the *Tetraselmis* sp. are almost completely mixed together. When α approaches 5, the main parts of the two cell streams can be separated, but under this condition, as shown in Figure 4C, the cell streams still have some overlap. When α approaches 10 or larger, the cell streams can be separated completely and the separation distance increase slowly as α does. In addition, compared with PFF, iPFF only needs to work at a smaller flow rate ratio ratio, which can increase cell flux significantly [31].

Theoretically, the cells (both *Tetraselmis* sp. and *Chlorella* sp.) cannot be focused to a thin layer close to one sidewall of the T-shaped channel when the flow rate ratio is small, such as 0.2, 1 or 5. So distribution ranges of *Tetraselmis* sp. and *Chlorella* sp. are very wide, especially in the abruptly broadened segment. As a result, the separation effect is undesirable. When α approaches 10 or larger, most cells are focused to the sidewall. Then the flow-induced inertial lift force pushes the cells towards to the central of the microchannel. The *Tetraselmis* sp. can be moved to the central line due to their large size while the *Chlorella* sp. still flows near the sidewall. Consequently, the two cells can be completely separated at this condition. Because of the large size deviation of the two types of cells (cells are in different life cycle stages) used in the experiment, though complete separation can be achieved, the cell separation does not show a most visible enhancement when the flow rate ratio is increased from 5 to 15.

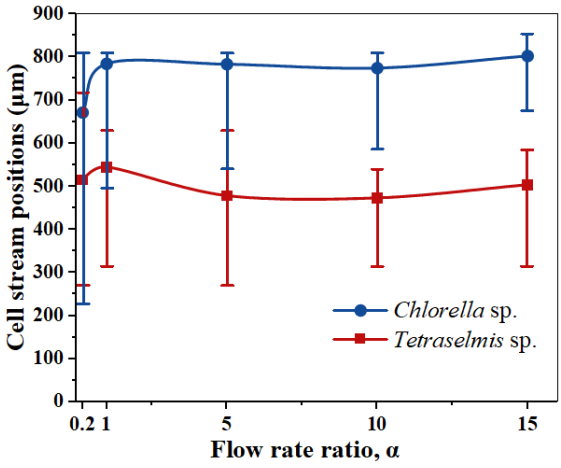

Figure 5. The effects of the flow rate ratio (α) on the stream positions for the *Chlorella* sp. (blue circle) and *Tetraselmis* sp. (red square). The bottom sidewall of the channel expansion was used as the reference point (0 μm).

4 Conclusions

It is a great challenge to detect the microalgae in the ballast water directly. So the separation of the microalgae according to size is necessary before detecting. Unfortunately, the methods for microalgae separation are not developed smoothly. In this study, a method to separate microalgae by inertia-enhanced pinched flow fractionation (iPFF) was proposed. Two types of microalgae, *Chlorella* sp. and *Tetraselmis* sp., were used in the experiment to study the performance of the method. The experimental results show that the separation effect becomes better at first but then remains unchanged when the Reynolds number in the microchannel increases. In addition, the separation effect becomes better with increasing the flow rate ratio between sheath fluid and microalgae mixture. In general, this study provides a simple method to separate the microalgae with different size. Besides a simple microfluidic chip, the method need only two syringe pumps which are easy to achieve in the laboratory or work shop. Next, several sets of electrodes would be fabricated on the bottom of the microfluidic channel where the microalgae are just separated by iPFF. In addition,

viscoelastic fluids will be used in further experiments. Because cell separation via iPFF can be enhanced if viscoelastic fluids are employed, which may resolve the issue for cells with large size deviations [33, 34]. So the separated microalgae could be detected accurately and continuously which is useful for the port state officers to manage the ships' ballast water in the future. In brief, this work lays a foundation for the management of the ballast water.

Acknowledgements

This research was funded by National Key Research and Development Program of China (2017YFC1404603), Natural Science Foundation of China (51909019, 51979045), the Fundamental Research Funds for the Central Universities (3132019336, 3132020184) and the Innovative Researcher Training Projects of Dalian Maritime University (CXXM2019BS010).

Conflict of interest

The authors have declared no conflict of interest.

Data Availability Statement

The data that support the findings of this study are available from the corresponding author upon reasonable request.

5 References

[1] David, M., Perkovič, M. *Mar. Pollut. Bull.* 2004, *49*, 313–318.

[2] Doblin, M. A., Dobbs, F. C. *Mar. Pollut. Bull.* 2006, *52*, 259–263.

[3] Zhang, T., Hong, Z.-Y., Tang, S.-Y., Li, W., Inglis, D. W., Hosokawa, Y., Yalikun, Y., Li, M. *Lab. Chip* 2020, *20*, 35–53.

[4] Zeng, J., Deng, Y., Vedantam, P., Tzeng, T.-R., Xuan, X. J. Magn. Magn. Mater. 2013, 346, 118–123.

[6] Wang, Y., Wang, J., Wu, X., Jiang, Z., Wang, W. *ELECTROPHORESIS* 2019, *40*, 969–978.

[7] Jiang, X., Liu, S., Zhang, Y., Ji, Y., Sohail, A., Cao, C., Wang, P., Xiao, H. *Anal. Chem.* 2020, *92*, 12017–12025.

[8] He, Y.-C., Kong, F.-Z., Fan, L.-Y., Wu, J. Y., Liu, X.-P., Li, J., Sun, Y., Zhang, Q., Yang, Y., Wu, X.-J., Xiao, H., Cao, C.-X. *Anal. Chim. Acta* 2017, *982*, 200–208.

[9] Dong, Y.-C., Shao, J., Yin, X.-Y., Fan, L., Cao, C.-X. *J. Sep. Sci.* 2011, *34*, 1683–1691.

[10] Fakhfouri, A., Devendran, C., Collins, D. J., Ai, Y., Neild, A. 10.

[11] Lin, S., Zhi, X., Chen, D., Xia, F., Shen, Y., Niu, J., Huang, S., Song, J., Miao, J., Cui, D., Ding, X. *Biosens. Bioelectron.* 2019, *129*, 175–181.

[12] Zeming, K. K., Thakor, N. V., Zhang, Y., Chen, C.-H. *Lab. Chip* 2016, *16*, 75–85.

[13] Lin, S., Yu, Z., Chen, D., Wang, Z., Miao, J., Li, Q., Zhang, D., Song, J., Cui, D. *Small* 2020, *16*, 1903916.

[14] Lee, M.-L., Yao, D.-J. *Inventions* 2018, *3*, 40.

[15] Zhang, J., Chintalaramulu, N., Vadivelu, R., An, H., Yuan, D., Jin, J., Ooi, C. H., Cock, I. E., Li, W., Nguyen, N.-T. *Anal. Chem.* 2020, *92*, 11558–11564.

[16] Rzhevskiy, A. S., Razavi Bazaz, S., Ding, L., Kapitannikova, A., Sayyadi, N., Campbell, D., Walsh, B., Gillatt, D., Ebrahimi Warkiani, M., Zvyagin, A. V. *Cancers* 2019, *12*, 81.

[17] Yamada, M., Nakashima, M., Seki, M. *Anal. Chem.* 2004, *76*, 5465–5471.

[18] Lu, X., Xuan, X. *Anal. Chem.* 2015, *87*, 4560–4565.

[19] Lu, X., Xuan, X. *Anal. Chem.* 2015, *87*, 6389–6396.

345 [20] Ylbing, S. *Research on Laser Direct Writing System and its Lithography Properties*, p.
346 10.
347 [21] Liu, Z., Li, J., Yang, J., Song, Y., Pan, X., Li, D. *Microfluid. Nanofluidics* 2017, *21*, 4.
348 [22] Hongbin, Y., Guangya, Z., Siong, C. F., Shouhua, W., Feiwen, L. *Sens. Actuators B*
349 *Chem.* 2009, *137*, 754–761.
350 [23] Nieuwstadt, H. A., Seda, R., Li, D. S., Fowlkes, J. B., Bull, J. L. *Biomed. Microdevices*
351 2011, *13*, 97–105.
352 [24] Di Carlo, D., Irimia, D., Tompkins, R. G., Toner, M. *Proc. Natl. Acad. Sci.* 2007, *104*,
353 18892–18897.
354 [25] Nieuwstadt, H. A., Seda, R., Li, D. S., Fowlkes, J. B., Bull, J. L. *Biomed. Microdevices*
355 2011, *13*, 97–105.
356 [26] Li, D., Shao, X., Bostwick, J. B., Xuan, X. *Microfluid. Nanofluidics* 2019, *23*, 125.
357 [27] Squires, T. M., Quake, S. R. *Rev. Mod. Phys.* 2005, *77*, 977–1026.
358 [28] Jelly, T. O., Busse, A. *Int. J. Heat Fluid Flow* 2019, *80*, 108485.
359 [29] Yuan, D., Tan, S. H., Zhao, Q., Yan, S., Sluyter, R., Nguyen, N. T., Zhang, J., Li, W.
360 *RSC Adv.* 2017, *7*, 3461–3469.
361 [30] Nam, J., Namgung, B., Lim, C. T., Bae, J.-E., Leo, H. L., Cho, K. S., Kim, S. *J.*
362 *Chromatogr. A* 2015, *1406*, 244–250.
363 [31] Singh, J., Kumar, C. V. A. *Rheol. Acta* 2019, *58*, 709–718.
364 [32] Liu, C., Hu, G., Jiang, X., Sun, J. *Lab. Chip* 2015, *15*, 1168–1177.
365 [33] Lu, X., Liu, C., Hu, G., Xuan, X. *J. Colloid Interface Sci.* 2017, *500*, 182–201.
366 [34] Fei, T., Qiang, F., Chen, Q., Liu, C., Li, T., Sun, J. *Microfluid. Nanofluidics* 2019, 9.